Published in final edited form as:
Cell. 2010 February 5; 140(3): 338. doi:10.1016/j.cell.2010.01.001.

Double-stranded RNA-dependent Protein Kinase Links Pathogen Sensing with Stress and Metabolic Homeostasis

Takahisa Nakamura[1], **Masato Furuhashi**[1], **Ping Li**[1], **Haiming Cao**[1], **Gurol Tuncman**[1], **Nahum Sonenberg**[2], **Cem Z. Gorgun**[1], and **Gökhan S. Hotamisligil**[1]

[1] Department of Genetics & Complex Diseases, Harvard School of Public Health, Boston, MA 02115, USA

[2] Department of Biochemistry, McGill University, Montreal, Quebec H3G1Y6, Canada

SUMMARY

As chronic inflammation is a hallmark of obesity, pathways that integrate nutrient and pathogen sensing pathways are of great interest in understanding the mechanisms of insulin resistance, type 2 diabetes, and other chronic metabolic pathologies. Here, we provide evidence that double-stranded RNA dependent protein kinase (PKR) can respond to nutrient signals as well as endoplasmic reticulum (ER) stress and coordinate the activity of other critical inflammatory kinases such as the c-Jun N-terminal kinase (JNK) to regulate insulin action and metabolism. PKR also directly targets and modifies insulin receptor substrate and hence integrates nutrients and insulin action with a defined pathogen response system. Dietary and genetic obesity features marked activation of PKR in adipose and liver tissues and absence of PKR alleviates metabolic deterioration due to nutrient or energy excess in mice. These findings demonstrate PKR as a critical component of an inflammatory complex that responds to nutrients and organelle dysfunction.

INTRODUCTION

Metabolic diseases appear as clusters including obesity, insulin resistance, type 2 diabetes, and cardiovascular disease, and constitute a major global health problem with limited treatment options. In the past decade, it has been realized that the emergence of this cluster has strong inflammatory underpinnings (Hotamisligil, 2006). During the course of obesity, a broad array of inflammatory and stress responses are evoked in metabolic tissues, leading to chronic, low grade local inflammation which plays a central role in the inhibition of insulin receptor signaling and disruption of systemic metabolic homeostasis. This atypical state, which we refer to as metaflammation (Hotamisligil, 2006), involves immune and non-immune cells and the engagement of immune response pathways with nutrients and metabolites. However, the mechanistic basis of these extensive functional links and molecules that coordinate this network of responses remains to be understood.

If the nutrient and pathogen response systems were truly integrated, the involvement of pathogen sensors in metabolic regulation, especially during exposure to excess nutrients would be anticipated. Such anticipation has stimulated the pursuit of pattern recognition receptors

To whom correspondence should be addressed: Gökhan S. Hotamisligil, M.D., Ph.D., Department of Genetics and Complex Diseases, Harvard School of Public Health, Boston, MA 02115, Fax: 617 432 1941, Phone: 617 432 1950, ghotamis@hsph.harvard.edu.

(PRRs) such as the Toll-like receptors (TLRs) for a role in metabolism (Shi et al., 2006). Other than PRRs, there are only a few molecules that can assume such a role to carry the potential ability for direct recognition of pathogens and possess catalytic activity to directly couple to metabolic pathways. One such molecule is the double-stranded RNA-dependent protein kinase (PKR), which has been originally identified as a pathogen sensor and a proposed regulator of the innate immune response against viral infections in higher eukaryotes (Samuel, 1993). Virus-derived double-stranded RNA molecules are recognized and bound by PKR through the N-terminal double-stranded RNA-binding motifs, resulting in autophosphorylation through the activation of the intramolecular kinase domain (Garcia et al., 2006; Williams, 2001). Interestingly, in the context of infections, PKR can regulate or act in conjunction with major inflammatory signaling pathways that are implicated in metabolic homeostasis, including the c-Jun N-teminal kinase (JNK) and IκB kinase (IKK) (Bonnet et al., 2000; Goh et al., 2000; Takada et al., 2007). In metabolic disease, it is unclear how these and other inflammatory signaling molecules are coordinately regulated to disrupt metabolism. However, it is feasible to consider a model where these multiple signaling pathways act in concert by forming a response node or acting in complexes that yield to metabolic surplus.

Interestingly, among the very few substrates identified for the kinase activity of PKR, the major one is the eukaryotic initiation factor 2α (eIF2α), which regulates general protein synthesis (Holcik and Sonenberg, 2005; Ron and Walter, 2007). It has been postulated that PKR-mediated phosphorylation of eIF2α is a strategy to inhibit viral protein synthesis in host cells (Holcik and Sonenberg, 2005). However, in other context, inhibition of general translation through the same eIF2α phosphorylation represents a major arm controlling endoplasmic reticulum (ER) homeostasis (Ron and Walter, 2007). ER stress also plays an important role in the development of insulin resistance and diabetes, at least in part, by triggering JNK activity (Gregor and Hotamisligil, 2007; Ozcan et al., 2004). In both mouse and human, there is consistent and marked increase in phosphorylation of eIF2α and JNK activity in obese metabolic tissues (Gregor et al., 2009). Hence, coordination of protein synthesis through eIF2α and stress signaling through JNK likely represent a relevant mechanism in the integration of inflammatory signals with metabolic outcomes, especially in the context of nutrient and energy surplus. PKR features properties to coordinate pathogen responses, endoplasmic reticulum function, inflammatory signaling, and translational regulation. Hence, we postulate that PKR may represent a core component of a putative “metabolic inflammasome”. In other words, an integration mechanism for pathogen response and metabolic pathways that plays a critical role in obesity, insulin action, and type 2 diabetes by controlling the action of major players such as JNK, IKK and/or other mediators to regulate metabolic homeostasis.

RESULTS

PKR activity in obesity and metabolic stress

If PKR were involved in nutrient-induced inflammatory responses, it would be anticipated that its activity is altered in conditions of nutrient surplus. To explore whether PKR activation is altered in obesity and metabolic stress, we first examined a model of severe genetic obesity and insulin resistance resulting from leptin deficiency (*ob/ob*, also known as $Lep^{ob/ob}$). There was a striking increase in PKR activity, which was assessed by autophosphorylation level of PKR using ATP $[\gamma\text{-}^{32}P]$, in both white adipose tissue (WAT) and liver of *ob/ob* mice compared to lean controls (Figure 1A). Similarly, there was a significant upregulation of PKR activity in both WAT and liver tissues of mice fed with a high fat diet (Figure 1B). In both models, we also observed an increase in PKR protein and mRNA levels, consistent with the reported autoregulation of PKR expression upon stimulation of its activity (Figure 1A, 1B, S1A, and S1B) (Gusella et al., 1995; Samuel, 1993). However, there was only a minor regulation of skeletal muscle tissue PKR activity in the *ob/ob* model and no regulation was evident in dietary

obesity (Figure S1C and S1D). In adipose tissue, the principle source of increased PKR expression in dietary obesity was found in mature adipocyte fraction instead of stromal-vascular (SV) fraction (Figure S1A). Interestingly, and in addition to PKR itself, mRNA levels of some other interferon target genes were also increased in adipocytes of obese WAT and liver (Figure S1A and S1B). As these mice were maintained in a specific pathogen-free environment, activation of PKR likely involves metabolic signals associated with nutrient and energy excess.

To determine whether PKR activity is related to metabolic stress and triggered by a nutrient, we next used an *in vivo* lipid infusion system, which acutely increases circulating free fatty acids (FFA) and causes insulin resistance (Kim et al., 2004; Shi et al., 2006). In this setting, there was also a significant increase in PKR activity in lean mice following lipid exposure (Figure 1C). These results demonstrate that PKR is activated by nutrient excess and metabolic stress *in vivo*. Given that PKR activity is induced by lipid infusion, we next explored whether FFA itself can also activate PKR by treating primary-isolated mouse embryonic fibroblast cells (MEFs) with palmitic acid. As shown in Figure 1D, palmitic acid exposure resulted in PKR activation. Since TLR4 has been implicated in fatty acid response (Shi et al., 2006), we asked whether PKR activation by lipids involved this PRR. However, in TLR4-deficient primary MEFs, palmitic acid-induced PKR activation was also detected at levels similar to wild type controls (Figure S1E). These experiments demonstrated that PKR is activated by lipids *in vitro* and *in vivo*, and this activation is not dependent on TLR4.

PKR controls JNK activity in response to metabolic stress

JNK activity is modulated by PKR under several stress conditions (Goh et al., 2000). Since JNK activation is also related to fatty acid exposure and ER stress (Gao et al., 2004; Urano et al., 2000) and critical for insulin sensitivity (Hirosumi et al., 2002), we next examined the impact of PKR on fatty acid- and ER stress-mediated JNK activation. To assess effects of PKR-deficiency in cells, we selected to use MEFs from mice with a targeted mutation lacking the PKR kinase domain (Abraham et al., 1999). Treatment of these PKR-deficient ($Pkr^{-/-}$) and wild type ($Pkr^{+/+}$) control primary-isolated MEFs with palmitic acid demonstrated that this fatty acid failed to activate JNK in the absence of PKR (Figure 2A). In a similar fashion, treatment of $Pkr^{+/+}$ and $Pkr^{-/-}$ MEFs with thapsigargin, an agent that induced ER stress, resulted in prominent induction of JNK phosphorylation in $Pkr^{+/+}$ relative to $Pkr^{-/-}$ cells (Figure 2B). ER stress-induced PKR activation was decreased in the presence of translation inhibitor cycloheximide. Therefore, new protein synthesis, at least in part, appears to be required for PKR activation during ER stress (Figure S2A). Taken together, these results demonstrate that PKR is a required component for JNK activation in response to lipid exposure and ER stress.

One mechanism by which JNK negatively regulates insulin signaling is through induction of IRS-1 serine phophorylation in response to fatty acid exposure and ER stress (Gao et al., 2004; Ozcan et al., 2004). If PKR controls JNK activation, it is conceivable that PKR may, indirectly or directly, target IRS-1 function, which is critical in insulin action. To address whether fatty acid- or ER stress-induced IRS-1 phosphorylation is dependent on PKR, we examined the effect of palmitic acid or thapsigargin treatment on IRS-1 serine phosphorylation in $Pkr^{+/+}$ and $Pkr^{-/-}$ MEFs. Both of these treatments resulted in induction of IRS-1 serine 307 phosphorylation in $Pkr^{+/+}$ MEFs but not in $Pkr^{-/-}$ cells (Figure 2C and 2D). As these data suggest that activated PKR modulates IRS-1 serine phosphorylation, we next assessed the effect of a direct PKR activator, a virus-derived double stranded RNA mimetic, polyinosinic-polycytidylic acid (PolyI•C) (Garcia et al., 2006; Williams, 2001), on IRS-1 phosphorylation in $Pkr^{+/+}$ and $Pkr^{-/-}$ MEFs. This treatment also induced IRS-1 serine phosphorylation with a marked increase in PKR expression in $Pkr^{+/+}$ MEFs.

However, polyI•C-induced IRS-1 phosphorylation was not observed in *Pkr*$^{-/-}$ MEFs (Figure S2B). We also reconstituted PKR expression in the *Pkr*$^{-/-}$ MEFs since increased PKR expression itself induces PKR activity thus allowing comparisons in the same cellular background without stimulation of other signaling pathways (Figure S2C). As shown in Figure 2E, serine phosphorylation of IRS-1 was induced by reconstitution of PKR in *Pkr*-deficient cells. In these cells, the level of insulin-induced tyrosine phosphorylation of IRS-1 and insulin-induced interaction between IRS-1 and p85, a regulatory subunit of phosphoinositide 3-kinase (PI3K), were both significantly diminished in PKR-reconstituted cells compared to the *Pkr*$^{-/-}$ controls expressing the empty vector (Figure 2F). Hence, PKR can induce IRS serine phosphorylation and block insulin action.

We next asked whether RNA binding ability of PKR is required for palmitic acid- or ER stress-induced PKR activation. RNA binding capacity of PKR is abolished by introducing a point mutation to its lysine 64 residue in the RNA binding motif (McCormack et al., 1994; Wu and Kaufman, 1996). We reconstituted *Pkr*$^{-/-}$ MEFs with wild type (WT) or RNA binding defective (K64E) PKR by retrovirus-mediated gene transfer, and examined PKR kinase activity after treatment with palmitic acid or thapsigargin. Wild type PKR is activated by both palmitic acid and thapsigargin (Figure 2G and 2H). However, PKR with defective RNA binding (K64E) was not activated in palmitic acid- or thapsigargin-treated cells (Figure 2G and 2H). A mutation in the kinase domain of PKR abolished all activity and was used as a control (Figure 2G and 2H). These data demonstrate that PKR is a required component for JNK activation and IRS-1 inhibition when induced by a nutrient, a pathogen component or ER stress, and the RNA binding domain of PKR is indispensable in both responses.

IRS-1, a novel and direct substrate of PKR

We next treated *Pkr*$^{+/+}$ and *Pkr*$^{-/-}$ cells with TNFα, which is well known to induce both PKR activity and block insulin action through IRS-1 phosphorylation in wild type cells (Hotamisligil et al., 1996). In these experiments, we noticed that PKR was detectable by western blot analysis following immunoprecipitation with an anti-IRS-1 antibody, demonstrating a potential interaction between these proteins (Figure 3A). To verify the interaction between PKR and IRS-1, we next performed the reciprocal experiment, where we immunoprecipitated PKR from protein extracts of TNFα-treated *Pkr*$^{+/+}$ MEFs and attempted to detect IRS-1 by western blot analysis. PKR-deficient cells were used in the same setting as controls. These experiments also demonstrated the interaction between these two proteins (Figure 3B). To assess the specificity of PKR-IRS-1 interaction, we also examined the relation between IRS-1 and the PKR-like endoplasmic reticulum kinase (PERK), which is the closest homologue of PKR in mammals, and did not detect any interaction between these proteins with or without induction of ER stress (Figure S3).

We next performed an *in vitro* pull down assay using recombinant IRS-1 and PKR proteins. These experiments demonstrated that PKR directly interacts with IRS-1 protein (Figure 3C). The robust interaction between PKR and IRS-1 raised the possibility that PKR phosphorylates IRS-1 directly. To address this possibility, we performed kinase assays using recombinant IRS-1 and active PKR *in vitro*. As shown in Figure 3D, PKR directly phosphorylates IRS-1 including the serine 307 residue. We next performed *in vitro* kinase assays after immunopurification of PKR from *Pkr*$^{+/+}$ MEFs and used *Pkr*$^{-/-}$ cell extracts as a negative control. We found that IRS-1 was phosphorylated by immunopurified PKR from TNFα- or thapsigargin-treated *Pkr*$^{+/+}$ MEFs (Figure 3E and 3F). More importantly, the increased serine phosphorylation of IRS-1, which is detected by a phospho-specific antibody, was induced only by activated PKR (Figure 3E and 3F). Again, the induction of IRS-1 phophorylation was not observed in extracts prepared from TNFα- or thapsigargin-treated *Pkr*$^{-/-}$ cells in control experiments (Figure 3E and 3F). We have previously shown that JNK1 plays a critical role in

stress-induced IRS-1 phosphorylation and insulin resistance (Hirosumi et al., 2002). To address whether JNK1 is required for PKR-mediated IRS-1 phosphorylation, we next assessed effects of exogenous expression of PKR on IRS-1 phosphorylation in primary $Jnk1^{+/+}$ and $Jnk1^{-/-}$ MEFs. By introducing PKR through adenovirus-mediated gene transfer, serine phosphorylation of IRS-1 is dramatically increased in $Jnk1^{+/+}$ MEFs (Figure 3G). In $Jnk1^{-/-}$ MEFs, PKR still retained the ability to induce serine phosphorylation of IRS-1 (Figure 3G), although this was significantly reduced in magnitude. These data suggest that PKR assumes a role in regulation of IRS-1 phosphoryation in both JNK1-dependent and -independent manner in cultured cells and illustrate the importance of functional interaction between these kinases to interfere with insulin action.

Metabolic regulation and insulin action in $Pkr^{-/-}$ mice

Given that PKR activity is strongly regulated in obesity and linked to signaling pathways interfering with metabolic homeostasis, we then tested the functional significance of PKR in the pathogenesis of obesity, insulin resistance and type 2 diabetes using several different *in vivo* models. First, mice lacking PKR ($Pkr^{-/-}$) and wild type control ($Pkr^{+/+}$) were placed on a high fat diet (HFD) along with a control group of each genotype on regular diet (RD). The PKR-deficient model used in our study was generated by removing the kinase domain hence retains no kinase activity (Abraham et al., 1999). On HFD, $Pkr^{+/+}$ mice developed obesity compared to mice kept on RD, while weight gain in $Pkr^{-/-}$ mice was significantly lower, starting to become evident after 10 weeks of HFD (Figure 4A). Dual energy X-ray absorption (DEXA) analysis demonstrated reduced total body adipose mass in $Pkr^{-/-}$ mice (Figure 4B). In addition, consistent with reduced adiposity, serum leptin level in $Pkr^{-/-}$ mice was lower than that in $Pkr^{+/+}$ mice (Figure 4C). Total serum adiponectin levels were not significantly different between genotypes (Figure 4D). In $Pkr^{-/-}$ mice, blood glucose level was significantly lower than those in $Pkr^{+/+}$ controls (Figure 4E). Examination of serum insulin level revealed that the hyperinsulinemia observed in $Pkr^{+/+}$ mice was not evident in the $Pkr^{-/-}$ animals, indicating that these animals might exhibit enhanced insulin sensitivity (Figure 4F). To investigate systemic insulin sensitivity, we performed glucose tolerance tests (GTT) in $Pkr^{-/-}$ and $Pkr^{+/+}$ mice at 6 and 14 weeks after the start of HFD. Since body weights of $Pkr^{+/+}$ and $Pkr^{-/-}$ mice did not exhibit significant differences until week 10–12, experiments performed at an early stage allowed evaluation of insulin sensitivity without changes in body weight. After 6 weeks of HFD, where the body weights were similar between genotypes, $Pkr^{-/-}$ mice already showed significantly lower glucose levels after a glucose challenge compared to $Pkr^{+/+}$ mice (Figure 4G). This increased glucose tolerance continued to be evident in $Pkr^{-/-}$ mice after 14 weeks of HFD (Figure S4A). Similarly, during insulin tolerance tests (ITT), the hypoglycemic response to insulin was also significantly enhanced in $Pkr^{-/-}$ mice compared to $Pkr^{+/+}$ controls after 16 weeks of HFD (Figure S4B). Glucose disposal curves and the hypoglycemic response to insulin in mice on RD were similar between genotypes (Figure S4C and S4D). Although no significant changes were observed in heat production, food intake, or total physical activity between genotypes (Figure S4E–S4H), rates of oxygen consumption and carbon dioxide production of $Pkr^{-/-}$ mice were modestly but significantly higher than those of $Pkr^{+/+}$ mice (Figure S4I and S4J), indicating that energy expenditure may be a potential mechanism for body weight reduction.

Biochemical and molecular alterations in $Pkr^{-/-}$ mice

We next studied whether deficiency of PKR resulted in enhanced insulin action by examining *in vivo* insulin receptor-signaling capacity in WAT and liver tissues of mice on HFD. In intact animals, insulin-stimulated AKT phosphorylation on serine 473 was significantly increased in WAT extracts of $Pkr^{-/-}$ mice compared with that of $Pkr^{+/+}$ controls (Figure 5A). There was also significantly increased insulin-stimulated AKT phosphorylation in liver tissue of $Pkr^{-/-}$ mice (Figure 5B). On the other hand, we did not observe significant alterations in insulin

signaling in the skeletal muscle of $Pkr^{-/-}$ mice (Figure S5A). These results demonstrate significant contribution of PKR to high fat diet-induced insulin resistance. Since eIF2α is a substrate of PKR, we determined the phosphorylation level of eIF2α on Ser52 using a specific antibody. These experiments demonstrate markedly decreased eIF2α phosphorylation in both adipose tissue and liver extracts of $Pkr^{-/-}$ mice compared with those of $Pkr^{+/+}$ controls (Figure 5C and 5D). Dietary obesity is also characterized by increased JNK activity (Hirosumi et al., 2002), which is correlated with PKR activity (Figure 1). In liver and adipose tissues, JNK1 activity was significantly reduced in $Pkr^{-/-}$ mice compared with $Pkr^{+/+}$ controls on HFD (Figure 5C, 5D, and S5B). These biochemical alterations were also reflected on the expression of inflammatory mediators induced by obesity in adipose tissue. In $Pkr^{-/-}$ mice, expression levels of several inflammatory cytokines such as *Tnfa*, *Il6*, and *Il1b*, and an anti-inflammatory cytokine *Il10*, *a* potential target of PKR (Chakrabarti et al., 2008), were significantly reduced in comparison to levels seen in $Pkr^{+/+}$ controls on HFD (Figure 5E). In addition, expression of a macrophage marker *F4/80* and an ER stress marker *Grp78* was also significantly reduced in adipose tissue of $Pkr^{-/-}$ mice (Figure 5E). These changes in gene expression between genotypes were not observed in mice fed RD (Figure S5C). Consistent with the HFD-induced changes in inflammatory gene expression, examination of the WAT sections revealed reduced inflammatory cells in $Pkr^{-/-}$ mice compared to $Pkr^{+/+}$ controls (Figure 5F). There was also a reduction in hepatic fatty infiltration (Figure 5G). Biochemical measurement of liver triglycerides demonstrated the reduction in liver lipid content in $Pkr^{-/-}$ mice (Figure 5H). Serum alanine aminotransferase (ALT) level was not significantly different between genotypes (Figure 5I).

A role of PKR in lipid infusion-induced acute insulin resistance

As shown in Figure 1, lipid exposure leads to PKR activation. To further explore the impact of PKR on insulin sensitivity in another setting and without the potential confounding effects of body weight or adiposity, we studied the effects of PKR activation on acute insulin resistance induced by lipids (Shi et al., 2006). In this system, we administered lipid intravenously into the $Pkr^{+/+}$ and $Pkr^{-/-}$ mice on regular diet, and performed hyperinsulinemic-euglycemic clamp studies to examine the whole body insulin sensitivity and glucose metabolism. Glucose infusion rates (GIR) during the clamp studies indicated that $Pkr^{-/-}$ mice required significantly higher levels of glucose infusion to maintain blood glucose consistent with increased insulin sensitivity (Figure 6A). In $Pkr^{+/+}$ mice, GIR required to maintain euglycemia was reduced by 50.2% in comparison with saline-infused controls (Figure 6B). In contrast, lipid infusion exerted a significantly smaller effect on the GIR in $Pkr^{-/-}$ mice (Figure 6B). Consistent with this result, the whole-body glucose disposal rates (Rd) observed in $Pkr^{-/-}$ mice during the clamp were significantly higher than those in $Pkr^{+/+}$ controls (Figure 6C). A similar trend was also observed in hepatic glucose production (HGP) levels, although this did not reach statistical significance (Figure 6D). Examination of insulin-stimulated tissue glucose uptake revealed significant increase in muscle tissue of $Pkr^{-/-}$ mice compared to $Pkr^{+/+}$ controls (Figure 6E). Although WAT glucose uptake was not significantly different between genotypes, a similar trend was also observed (Figure 6F). Under these conditions, lipid infusion did not result in differential activation of pro-apoptotic pathways between genotypes, indicating that the reported apoptotic activity of PKR was not an underlying contributor to the phenotype seen in the $Pkr^{-/-}$ mice (Figure S6). Taken together these data clearly show that lipid-induced PKR activation is an important negative regulator of insulin action and that PKR directly regulates insulin sensitivity in multiple settings.

DISCUSSION

While the integration of nutrient and pathogen response systems has been put forward as an attractive model to explain the inflammatory origin of metabolic disease, identification of

specific molecules and mechanisms directly coordinating these extensive links has been a major challenge (Hotamisligil and Erbay, 2008). In this study, we uncovered a link between an established pathogen-sensing pathway mediated by PKR and metabolic homeostasis through regulation of JNK activity and insulin action (Figure 7). This raises an intriguing possibility that PKR may act as a central integrator in the inflammatory component of metabolic control by linking nutrient- and pathogen-sensing pathways.

One of the remaining important questions regarding the relationships between inflammatory pathways and insulin action is how many molecules with similar biological functions are coordinated. Previous studies have shown direct interactions of PKR with the IKKβ-NF-κB pathway (Bonnet et al., 2000). In this study, we have demonstrated PKR's direct interaction and modulation of IRS, a critical molecule in insulin action, and the major regulatory role over JNK activation. Taken together, these findings make PKR a very attractive molecule at the core of a complex that features major inflammatory and stress roads that intersect with metabolism. Since activation of several stress signaling pathways produces similar outcomes in metabolic regulation, the possibility that these molecules work as part of a complex or a signaling node assembled and coordinated by a molecule of innate immunity with direct nutrient recognition potential is of critical importance. Such a role is highlighted for PKR in the integration of nutrient and pathogen sensing in relation to metabolic homeostasis (Figure 7). In this scenario, it is possible that the activity of one component is highly regulated by the other and thus amplified feedback mechanisms may be in place. For example, the interaction and function of JNK or IKK may also influence PKR and PKR activation, in turn contributing to organelle stress. Hence, we suggest that PKR may be critical in the assembly and activation of a putative metabolic inflammasome (or metaflammasome). These interesting possibilities merit further investigation.

It is noteworthy that PKR responds to pathogens, nutrients, and organelle stress. Then, PKR plays a role in the mounting of adaptive and survival responses including suppression of general protein translation through phosphorylation of eIF2α and inhibition of anabolic effects of insulin action. The marked increase in PKR activity observed in multiple models of obesity featuring energy and nutrient excess may represent an adaptive attempt to interfere with synthetic pathways that would further accumulate energy. This is consistent with the late onset effects of PKR activity on adiposity. The function of PKR activation may be limited to coordinated launching of an inflammatory response together with kinases such as JNK and IKK, as supported by the evidence provided in this study, which results in alterations in insulin action and possibly other metabolic outcomes. The most attractive implication of our observation is that PKR can directly sense nutrients or other metabolic products including endogenous RNA species produced during metabolic or ER stress. This possibility is strongly supported by the observation that PKR's defined RNA binding domain is required for its activation by lipids or ER stress (Figure 2G and 2H).

On the other hand, PKR's ability to sense and respond to pathogens directly and to control the inflammatory output and metabolic consequences illustrates the diversity of PKR-mediated responses to both extrinsic and intrinsic stress signals. This functional diversity also raises the possibility that the role of PKR in metabolic regulation may not only be critical in dietary exposures and insulin resistance, but may also include other metabolic abnormalities that emerge during the course of certain infections. For example, both type 1 and type 2 diabetes have been associated with viral infections, but mechanisms linking viral infections to diabetes are not well understood (Antonelli et al., 2009; von Herrath, 2009). It is known that one-third of patients with chronic hepatitis C, which can trigger PKR activity, develop type 2 diabetes (Bahtiyar et al., 2004; Delhem et al., 2001; Tokumoto et al., 2007). Molecular mechanisms by which β-cells are destroyed during the development of type 1 diabetes have also remained elusive although recent studies suggest a potential involvement of metabolic status, ER stress

and inflammatory responses (Eizirik et al., 2008; Ron and Walter, 2007). As PKR modifies insulin signaling and contributes to apoptosis induced by double stranded RNA (Scarim et al., 2001), it may offer critical insights into the pathogenesis of both forms of diabetes and metabolic deregulation triggered by viral infections.

Taken together with the previous reports, our results showing that PKR can act in conjunction with major inflammatory kinases and directly interact with a critical insulin signaling component lead us to suggest PKR as a core component of a putative "metabolic inflammasome" which consists of major elements in inflammatory signaling and insulin action (Figure 7). This PKR-coordinated sensing and signaling complex may represent a central mechanism for the integration of pathogen response and innate immunity with insulin action and metabolic pathways that are critical in chronic metabolic diseases. If small molecules can modulate *in vivo* PKR activity, therapeutic opportunities may arise from such efforts.

EXPERIMENTAL PROCEDURE

Mice

Animal care and experimental procedures were performed with approval from animal care committees of Harvard University. Two different types of targeted mutations of PKR have been established and reported in mice, RNA-binding domain defective and kinase-domain defective models (Abraham et al., 1999; Baltzis et al., 2002; Yang et al., 1995). In this study, the kinase-domain defective PKR-deficient mice have been used. Male $Pkr^{+/+}$ and $Pkr^{-/-}$ mice in the 129Sv × BALB/C mixed background (Abraham et al., 1999) were kept on a 12-h light/12-h dark cycle and were placed on a high-fat diet (D12492: 60% kcal% fat; Research Diets), beginning at 3 weeks of age *ad libitum*. After 6 and 14 weeks on HFD, GTTs were performed by intraperitoneal glucose injection (1.5 g/kg) following an overnight food withdrawal. After 16 weeks on HFD, ITTs were performed by intraperitoneal insulin injection (1 IU/kg) following 6 hours daytime food withdrawal. After 20 weeks, these mice were sacrificed and tissues were collected for further analysis. Total body fat mass was assessed by dual energy X-ray absorptiometry (DEXA; PIXImus). For metabolic measurements, mice were placed in an indirect open circuit calorimeter (Columbus Instruments). Serum insulin, leptin, and adiponectin levels were measured with ELISA (Alpco). Liver triglycerides were determined with a colorimetric system (Sigma-Aldrich) adapted for microtitre plate assays (Furuhashi et al., 2007). Serum alanine aminotransferase level was measured with Piccolo-lipid panel plus (Abaxis).

Hyperinsulinemic-euglycemic clamp studies

Hyperinsulinemic-euglycemic clamps were conducted as previously described (Furuhashi et al., 2007). For the lipid-induced acute insulin resistance mouse model, six-month-old male $Pkr^{+/+}$ and $Pkr^{-/-}$ mice were anesthetized and the right jugular vein was catheterized with a PE-10 polyethylene tube filled with heparin solution (100 U/ml) (United States Pharmacopeia). After a 3-day recovery, overnight-fasted mice were preinfused with lipid (5 ml/kg/h; Intralipid; Baxter Healthcare Corporation) or saline for 3 hours followed by further infusion with HPLC purified ^{3}H-glucose (0.05 μCi/min; Perkin Elmer) for 2 hours basal period. The Intralipid we used contains 20% Soybean Oil. The Soybean oil is a refined natural product consisting of a mixture of neutral triglycerides of predominantly linoleic, oleic, palmitic, linolenic, and stearic acids. After the basal period, a 120 min hyperinsulinemic-euglycemic clamp was conducted with a primed-continuous infusion of human insulin (Novolin; Novo Nordisk) at a rate of 12.5 mU/kg/min. Blood samples were collected at 20 min intervals for the immediate measurement of plasma glucose concentration, and 25% glucose was infused at variable rates to maintain plasma glucose at basal concentrations. Insulin-stimulated whole-body glucose disposal was estimated with a continuous infusion of ^{3}H-glucose throughout the clamps (0.1μCi/min). To

estimate insulin-stimulated glucose uptake in individual tissues, 2-^{14}C-deoxyglucose (2-^{14}C-DG; Perkin Elmer) was administered as a bolus (10 μCi) 75 min after the start of clamps. Blood samples were collected for the determination of plasma ^{3}H-glucose, $^{3}H_2O$, and 2-^{14}C-DG concentrations. At the end of clamps, muscles from both hindlimbs and epididymal adipose tissue were harvested and immediately frozen in liquid N_2 and stored at −80°C until further analysis. Calculations for the determination of metabolic parameters are described in the Supplemental Data.

Portal vein insulin infusion and protein extraction from tissues

Following 6 hour food withdrawal, mice were anesthetized and insulin (2 IU/kg) or PBS was injected into mice through the portal vein. Three minutes after injection, tissues were removed, frozen in liquid nitrogen, and kept at −80°C until processing. For protein extraction, tissues were placed in a cold lysis buffer [25 mM Tris-HCl (pH 7.4), 1 mM EGTA, 1 mM EDTA, 10 mM $Na_4P_2O_7$, 10 mM NaF, 2 mM Na_3VO_4, 1% NP-40, 1 mM PMSF, 1% protease inhibitor cocktail (Sigma-Aldrich)]. After homogenization on ice, the tissue lysates were centrifuged, and the supernatants were used for western blot analysis.

MEF culture and analysis

Primary *Pkr*$^{+/+}$ and *Pkr*$^{-/-}$ MEFs were used to assess phosphorylated JNK level or JNK activity under palmitic acid, TNFα, Thapsigargin, or polyinosinic-polycytidylic acid stimulation. Both *Pkr*$^{+/+}$ and *Pkr*$^{-/-}$ cell lines were established using the standard 3T3 immortalization protocol and used to assess phosphorylation level of IRS-1 and effects of PKR reconstitution on insulin action. At 70–80% confluency, cells were serum depleted for 3 hours or overnight prior to the stimuli. Sodium palmitate was dissolved in water at 65°C and prepared as 20 mM solution. In cell culture experiments, the 20 mM palmitic acid preparation was diluted with 0.5% BSA containing DMEM to obtain the 0.5 mM palmitic acid concentration. Reagents and recombinant cytokines were gently added to the culture dishes in the incubator to prevent any environmental stress. For retrovirus production, BOSC23 packaging cells were transfected at 70% confluence with Lipofectamine 2000 (Invitrogen) and a retroviral vector containing flag-tagged human PKR coding region. After 48 hours, the viral supernatant was harvested and filtered. Cells were incubated overnight with the viral supernatant, supplemented with 8 μg/mL polybrene. Expression vectors of adenovirus were constructed by cloning flag-tagged human PKR in adenovirus vector pAD/CMV/V5-DEST and the viruses were produced as described in Virapower adenovirus system (Invitrogen). Amplified-virus was used to infect primary *Jnk1*$^{+/+}$ and *Jnk1*$^{-/-}$ MEFs.

Kinase assays

Tissue or cell lysates containing 100–300 μg of protein were mixed with agarose-conjugated PKR antibody (Santa Cruz). The mixture was agitated at 4°C, pelleted by centrifugation and washed with lysis buffer followed by additional washes with PKR kinase buffer [15 mM Hepes (pH7.4), 10 mM $MgCl_2$, 40 mM KCl, 2 mM DTT] for equilibration. The beads were incubated in kinase buffer containing 10 μCi ^{32}P-γATP (PerkinElmer) at 30°C for 20 min followed by SDS-PAGE. To assess the phosphorylation of IRS-1 by PKR, *in vitro* kinase assays were performed with anti-PKR immunoprecipitates from lysates of *Pkr*$^{+/+}$ and *Pkr*$^{-/-}$ MEFs, which were treated by TNFα or Thapsigargin. The anti-PKR immunoprecipitates were mixed with IRS-1, which was immunopurified with anti-IRS-1 antibody (Upstate Biotechnology) from serum-starved wild-type MEFs. Further procedures are provided in the Supplemental information.

Quantitative real-time PCR analysis

Total RNA was isolated using Trizol reagent (Invitrogen). For reverse transcription, total RNA was converted to first strand cDNA using a high capacity cDNA reverse transcription system (Applied Biosystems). Quantitative real-time PCR analysis was performed using SYBR Green in a real-time PCR machine (7300 Real Time PCR system; Applied Biosystems). Primers are listed in Supplementary Table 1. To normalize expression data of WAT and liver, 36B4 and GAPDH mRNAs were used as an internal control gene, respectively.

Statistical analysis

Experimental results were shown as the mean ± SEM. The mean values for biochemical data from each group were compared by Student's *t*-test. Comparisons between multiple time points were analyzed using repeated-measures analysis of variance, ANOVA. In all tests, $P < 0.05$ was considered significant.

Supplementary Material

Refer to Web version on PubMed Central for supplementary material.

Acknowledgments

We thank all members of the Hotamisligil lab for their scientific input and contributions, especially Brenna Baccaro, Sara Vallerie, Margaret F. Gregor, and Ling Yang for support and discussions and Kristen Gilbert, Rebecca Foote, and Julie Gound for administrative assistance. We are grateful to Jun Eguchi and Atsuo Sasaki for helpful discussions. This study is supported by a grant from the National Institutes of Health (to G.S.H). T.N. is supported by fellowships from the International Human Frontier Science Program and the Uehara Memorial Foundation. M.F. is supported by fellowships from the Japan Society for the Promotion of Science and the American Diabetes Association. H.C. is supported by a NIH Roadmap Fellowship (DK71507-04) and the American Diabetes Association.

References

Abraham N, Stojdl DF, Duncan PI, Methot N, Ishii T, Dube M, Vanderhyden BC, Atkins HL, Gray DA, McBurney MW, et al. Characterization of transgenic mice with targeted disruption of the catalytic domain of the double-stranded RNA-dependent protein kinase, PKR. J Biol Chem 1999;274:5953–5962. [PubMed: 10026221]

Antonelli A, Ferri C, Ferrari SM, Colaci M, Sansonno D, Fallahi P. Endocrine manifestations of hepatitis C virus infection. Nat Clin Pract Endocrinol Metab 2009;5:26–34. [PubMed: 19079271]

Bahtiyar G, Shin JJ, Aytaman A, Sowers JR, McFarlane SI. Association of diabetes and hepatitis C infection: epidemiologic evidence and pathophysiologic insights. Curr Diab Rep 2004;4:194–198. [PubMed: 15132884]

Baltzis D, Li S, Koromilas AE. Functional characterization of pkr gene products expressed in cells from mice with a targeted deletion of the N terminus or C terminus domain of PKR. J Biol Chem 2002;277:38364–38372. [PubMed: 12161430]

Bonnet MC, Weil R, Dam E, Hovanessian AG, Meurs EF. PKR stimulates NF-kappaB irrespective of its kinase function by interacting with the IkappaB kinase complex. Mol Cell Biol 2000;20:4532–4542. [PubMed: 10848580]

Chakrabarti A, Sadler AJ, Kar N, Young HA, Silverman RH, Williams BR. Protein kinase R-dependent regulation of interleukin-10 in response to double-stranded RNA. J Biol Chem 2008;283:25132–25139. [PubMed: 18625702]

Delhem N, Sabile A, Gajardo R, Podevin P, Abadie A, Blaton MA, Kremsdorf D, Beretta L, Brechot C. Activation of the interferon-inducible protein kinase PKR by hepatocellular carcinoma derived-hepatitis C virus core protein. Oncogene 2001;20:5836–5845. [PubMed: 11593389]

Eizirik DL, Cardozo AK, Cnop M. The role for endoplasmic reticulum stress in diabetes mellitus. Endocr Rev 2008;29:42–61. [PubMed: 18048764]

Furuhashi M, Tuncman G, Gorgun CZ, Makowski L, Atsumi G, Vaillancourt E, Kono K, Babaev VR, Fazio S, Linton MF, et al. Treatment of diabetes and atherosclerosis by inhibiting fatty-acid-binding protein aP2. Nature 2007;447:959–965. [PubMed: 17554340]

Gao Z, Zhang X, Zuberi A, Hwang D, Quon MJ, Lefevre M, Ye J. Inhibition of insulin sensitivity by free fatty acids requires activation of multiple serine kinases in 3T3-L1 adipocytes. Mol Endocrinol 2004;18:2024–2034. [PubMed: 15143153]

Garcia MA, Gil J, Ventoso I, Guerra S, Domingo E, Rivas C, Esteban M. Impact of protein kinase PKR in cell biology: from antiviral to antiproliferative action. Microbiol Mol Biol Rev 2006;70:1032–1060. [PubMed: 17158706]

Goh KC, deVeer MJ, Williams BR. The protein kinase PKR is required for p38 MAPK activation and the innate immune response to bacterial endotoxin. Embo J 2000;19:4292–4297. [PubMed: 10944112]

Gregor MF, Yang L, Fabbrini E, Mohammed BS, Eagon JC, Hotamisligil GS, Klein S. Endoplasmic reticulum stress is reduced in tissues of obese subjects after weight loss. Diabetes 2009;58:693–700. [PubMed: 19066313]

Gregor MG, Hotamisligil GS. Adipocyte stress: The endoplasmic reticulum and metabolic disease. J Lipid Res 2007;48:1905–1914. [PubMed: 17699733]

Gusella GL, Musso T, Rottschafer SE, Pulkki K, Varesio L. Potential requirement of a functional double-stranded RNA-dependent protein kinase (PKR) for the tumoricidal activation of macrophages by lipopolysaccharide or IFN-alpha beta, but not IFN-gamma. J Immunol 1995;154:345–354. [PubMed: 7995954]

Hirosumi J, Tuncman G, Chang L, Gorgun CZ, Uysal KT, Maeda K, Karin M, Hotamisligil GS. A central role for JNK in obesity and insulin resistance. Nature 2002;420:333–336. [PubMed: 12447443]

Holcik M, Sonenberg N. Translational control in stress and apoptosis. Nat Rev Mol Cell Biol 2005;6:318–327. [PubMed: 15803138]

Hotamisligil GS. Inflammation and metabolic disorders. Nature 2006;444:860–867. [PubMed: 17167474]

Hotamisligil GS, Erbay E. Nutrient sensing and inflammation in metabolic diseases. Nat Rev Immunol 2008;8:923–934. [PubMed: 19029988]

Hotamisligil GS, Peraldi P, Budavari A, Ellis R, White MF, Spiegelman BM. IRS-1-mediated inhibition of insulin receptor tyrosine kinase activity in TNF-alpha- and obesity-induced insulin resistance. Science 1996;271:665–668. [PubMed: 8571133]

Kim JK, Fillmore JJ, Sunshine MJ, Albrecht B, Higashimori T, Kim DW, Liu ZX, Soos TJ, Cline GW, O'Brien WR, et al. PKC-theta knockout mice are protected from fat-induced insulin resistance. J Clin Invest 2004;114:823–827. [PubMed: 15372106]

McCormack SJ, Ortega LG, Doohan JP, Samuel CE. Mechanism of interferon action motif I of the interferon-induced, RNA-dependent protein kinase (PKR) is sufficient to mediate RNA-binding activity. Virology 1994;198:92–99. [PubMed: 7505074]

Ozcan U, Cao Q, Yilmaz E, Lee AH, Iwakoshi NN, Ozdelen E, Tuncman G, Gorgun C, Glimcher LH, Hotamisligil GS. Endoplasmic reticulum stress links obesity, insulin action, and type 2 diabetes. Science 2004;306:457–461. [PubMed: 15486293]

Ron D, Walter P. Signal integration in the endoplasmic reticulum unfolded protein response. Nat Rev Mol Cell Biol 2007;8:519–529. [PubMed: 17565364]

Samuel CE. The eIF-2 alpha protein kinases, regulators of translation in eukaryotes from yeasts to humans. J Biol Chem 1993;268:7603–7606. [PubMed: 8096514]

Scarim AL, Arnush M, Blair LA, Concepcion J, Heitmeier MR, Scheuner D, Kaufman RJ, Ryerse J, Buller RM, Corbett JA. Mechanisms of beta-cell death in response to double-stranded (ds) RNA and interferon-gamma: dsRNA-dependent protein kinase apoptosis and nitric oxide-dependent necrosis. Am J Pathol 2001;159:273–283. [PubMed: 11438474]

Shi H, Kokoeva MV, Inouye K, Tzameli I, Yin H, Flier JS. TLR4 links innate immunity and fatty acid-induced insulin resistance. J Clin Invest 2006;116:3015–3025. [PubMed: 17053832]

Takada Y, Ichikawa H, Pataer A, Swisher S, Aggarwal BB. Genetic deletion of PKR abrogates TNF-induced activation of IkappaBalpha kinase, JNK, Akt and cell proliferation but potentiates p44/p42 MAPK and p38 MAPK activation. Oncogene 2007;26:1201–1212. [PubMed: 16924232]

Tokumoto Y, Hiasa Y, Horiike N, Michitaka K, Matsuura B, Chung RT, Onji M. Hepatitis C virus expression and interferon antiviral action is dependent on PKR expression. J Med Virol 2007;79:1120–1127. [PubMed: 17596833]

Urano F, Wang X, Bertolotti A, Zhang Y, Chung P, Harding HP, Ron D. Coupling of stress in the ER to activation of JNK protein kinases by transmembrane protein kinase IRE1. Science 2000;287:664–666. [PubMed: 10650002]

von Herrath M. Can we learn from viruses how to prevent type 1 diabetes?: the role of viral infections in the pathogenesis of type 1 diabetes and the development of novel combination therapies. Diabetes 2009;58:2–11. [PubMed: 19114721]

Williams BR. Signal integration via PKR. Sci STKE 2001;2001:RE2. [PubMed: 11752661]

Wu S, Kaufman RJ. Double-stranded (ds) RNA binding and not dimerization correlates with the activation of the dsRNA-dependent protein kinase (PKR). J Biol Chem 1996;271:1756–1763. [PubMed: 8576179]

Yang YL, Reis LF, Pavlovic J, Aguzzi A, Schafer R, Kumar A, Williams BR, Aguet M, Weissmann C. Deficient signaling in mice devoid of double-stranded RNA-dependent protein kinase. EMBO J 1995;14:6095–6106. [PubMed: 8557029]

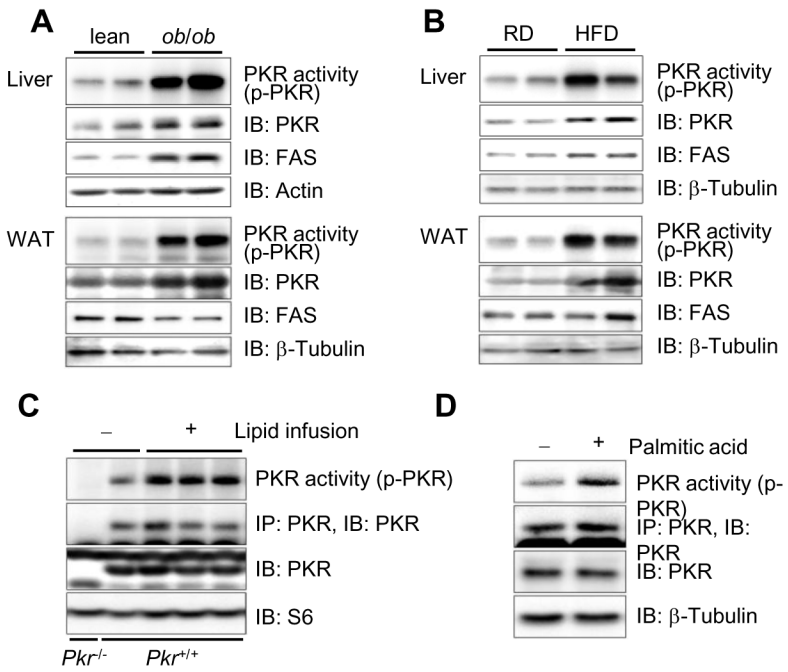

Figure 1. Regulation of PKR activity in obesity and lipid exposure

(A) A genetic mouse model of obesity (*ob/ob*) was used to examine PKR activity by a kinase assay using immunopurified PKR and ATP [γ-32P] in white adipose tissue (WAT) and liver compared with age- and sex- matched lean controls. Fatty acid synthase (FAS) and β-tubulin proteins are shown as controls.

(B) PKR activity was examined in white adipose tissue (WAT) and liver of the male wild type mice kept either on regular diet (RD) or high fat diet (HFD) for 20 weeks.

(C) PKR activity in liver of 10 week-old male wild type mice, which were infused with lipid or saline for 5 hours. Total S6 protein is shown as control.

(D) PKR activity in primary MEFs. Cells were cultured in the absence or presence of 0.5 mM palmitic acid for 2 hours.

See also Supplemental Figure S1.

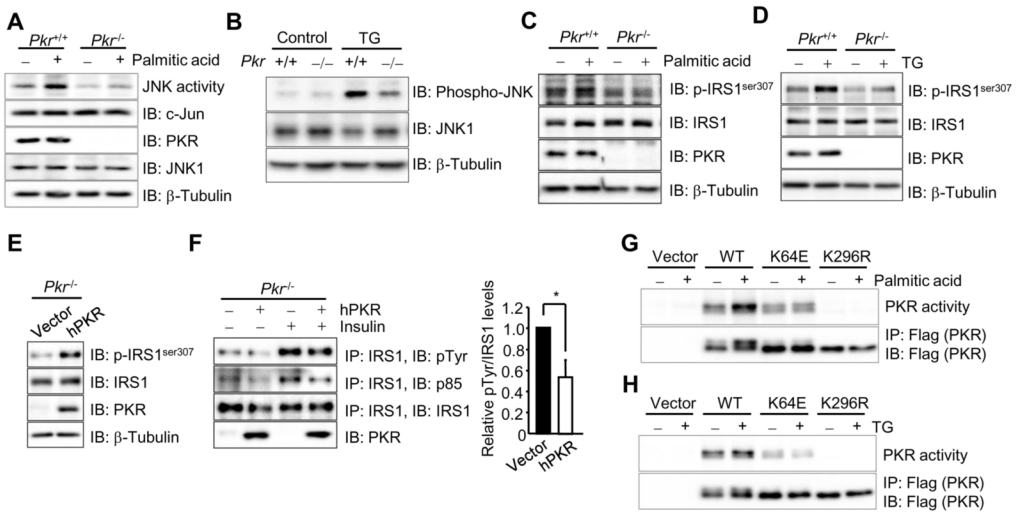

Figure 2. PKR regulates JNK activity resulting in inhibition of insulin signaling

(A) Primary $Pkr^{+/+}$ and $Pkr^{-/-}$ MEFs were treated with 0.5 mM palmitic acid for 2 hours. JNK activity was assessed by a kinase assay using recombinant c-Jun protein as substrate.

(B) Induction of JNK phosphorylation after 300 nM thapsigargin treatment for 1 hour in primary $Pkr^{+/+}$ and $Pkr^{-/-}$ MEFs. Phosphorylation level of JNK was examined with anti-phospho-JNK (Thr183/Tyr185) antibody.

(C and D) Induction of IRS-1 phosphorylation after 0.5 mM palmitic acid (C) or 300 nM thapsigargin (D) treatment for 2 hours in $Pkr^{+/+}$ and $Pkr^{-/-}$ MEFs. Phosphorylation level of IRS-1 on Ser307 was examined with anti-phospho-IRS-1 (serine 307) antibody.

(E) Induction of IRS-1 phosphorylation in retrovirally PKR-reconstituted $Pkr^{-/-}$ MEFs. The cells were serum-starved for 14 hours followed by western blot analysis with anti-phospho-IRS-1 (serine 307) antibody.

(F) The PKR-reconstituted $Pkr^{-/-}$ MEFs were stimulated with 10 nM Insulin for 3 minutes. The cell lysates were immunoprecipitated with anti-IRS-1 antibody followed by western blot analysis with anti-phospho-tyrosine and anti-PI3K (p85 subunit) antibodies. The graph on the right shows the quantification of the results. Data are shown as the mean ± SEM. $*P<0.05$.

(G and H) Induction of palmitic acid- and thapsigargin-induced PKR activity requires intact RNA binding domain of PKR. $Pkr^{-/-}$ MEFs were reconstituted with vector, flag-tagged wild type (WT), RNA binding domain mutant (K64E), or kinase dead mutant (K296R) of PKR by retrovirus-mediated gene transfer. These cells were maintained in serum-free DMEM containing 0.5% BSA for 14 hours followed by treatment with 0.5 mM palmitic acid for 90 minutes (G) or 300 nM thapsigardin for 1 hour (H). The cell lysates were immunoprecipitated with anti-Flag antibody followed by PKR kinase assay and western blot analysis with anti-Flag antibody.

See also Supplemental Figure S2.

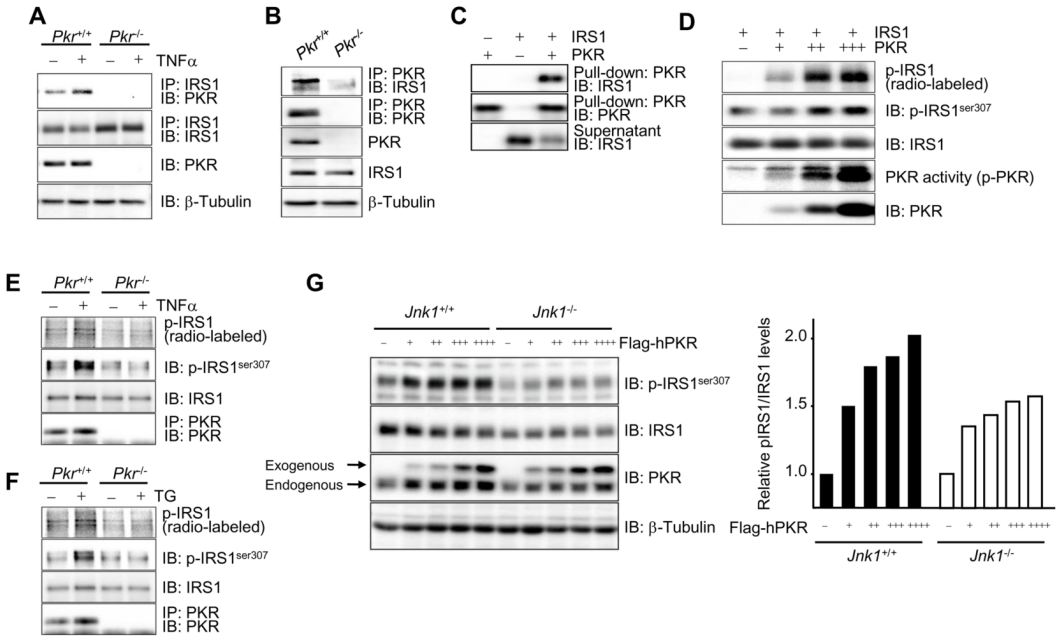

Figure 3. PKR directly regulates IRS-1 phosphorylation

(A) Induction of interaction between IRS-1 and PKR after TNFα treatment in *Pkr*$^{+/+}$ and *Pkr*$^{-/-}$ MEFs. IRS-1 and PKR protein level were examined either with immunoprecipitation (IP) followed by immunoblotting (IB) or by direct immunobloting in cells treated with 5 ng/ml TNFα treatment for 3 hours.

(B) Physical interaction between IRS-1 and PKR in TNFα-treated MEF cells. Cell lysates were prepared from *Pkr*$^{+/+}$ or *Pkr*$^{-/-}$ MEFs treated with 5 ng/ml TNFα for 3 hour followed by immunoprecipitation with anti-PKR antibody and western blot analysis with anti-IRS-1 antibody.

(C) Physical interaction between IRS-1 and PKR in a pull-down assay *in vitro* using recombinant IRS-1 and PKR proteins.

(D) Direct phosphorylation of IRS-1 by PKR in kinase assay *in vitro* using recombinant IRS-1 and PKR proteins. Phosphorylation level of IRS-1 was assessed by autoradiography or western blot analysis with anti-phospho-IRS-1 (serine 307) antibody.

(E and F) *In vitro* PKR kinase assay. IRS-1 phosphorylation by immunopurified PKR prepared from 5 ng/ml TNFα (E)- or 300 nM thapsigargin (F)-treated MEFs and analyzed by autoradiography or western blot analysis with anti-phospho-IRS-1 (serine 307) antibody.

(G) Effects of exogenous expression of PKR on IRS-1 serine phosphorylation in primary *Jnk1*$^{+/+}$ and *Jnk1*$^{-/-}$ MEFs. Flag-tagged human PKR was introduced to primary *Jnk1*$^{+/+}$ and *Jnk1*$^{-/-}$ MEFs by adenovirus-mediated gene transfer. Phosphorylation level of IRS-1 on serine 307 was examined with anti-phospho-IRS-1 (serine 307) antibody. Both exogenous and endogenous PKR expression was detected by anti-PKR antibody. The graph on the right shows the quantification of the data.

See also Supplemental Figure S3.

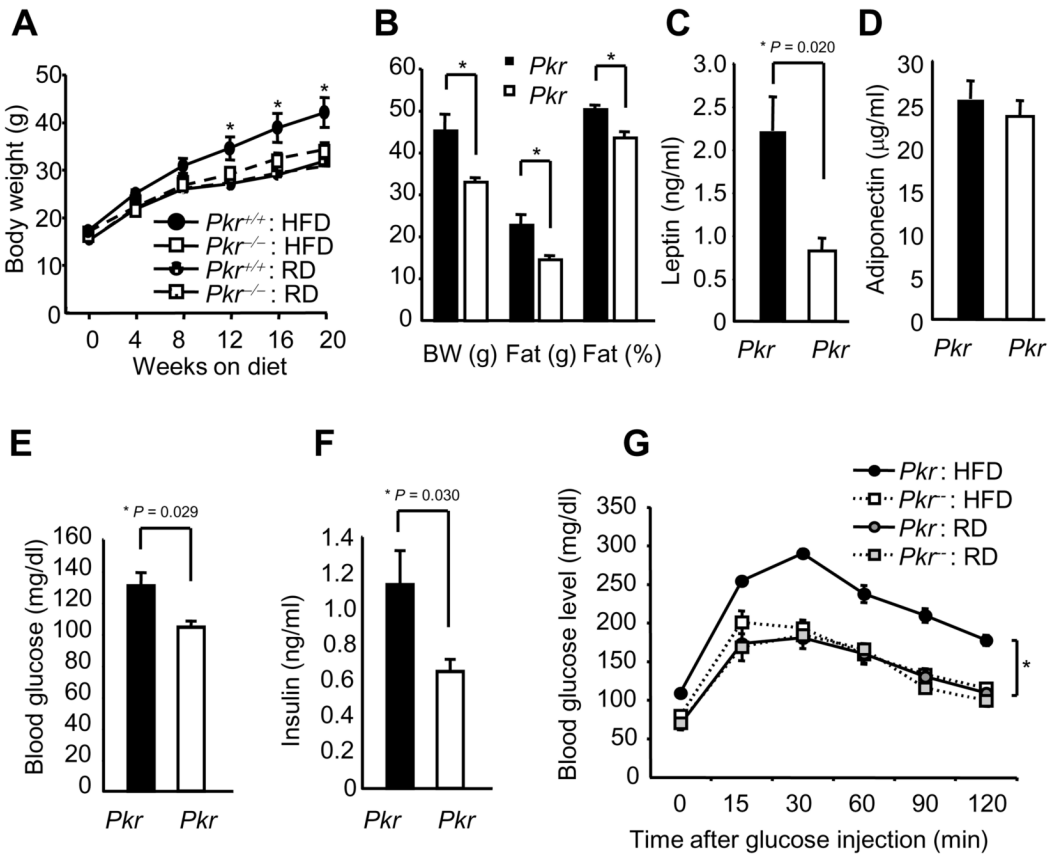

Figure 4. Glucose metabolism and insulin sensitivity in *Pkr*$^{-/-}$ mice

(A) Total body weight on regular (RD) or high fat (HFD) diet. Obesity is induced by HFD starting immediately after weaning at 3 weeks of age.

(B) Analysis of body fat by dual energy X-ray absorptiometry (DEXA).

(C and D) Serum leptin (C) and adiponectin (D) levels after 6 hours daytime food withdrawal in *Pkr*$^{+/+}$ (n = 5) and *Pkr*$^{-/-}$ (n = 6) mice on HFD for 15 weeks.

(E and F) Blood glucose (E) and serum insulin (F) levels after 6 hours daytime food withdrawal in *Pkr*$^{+/+}$ (n = 6) and *Pkr*$^{-/-}$ (n = 6) mice on HFD for 8 weeks.

(G) Glucose tolerance tests were performed on *Pkr*$^{+/+}$ (n = 6) and *Pkr*$^{-/-}$ mice (n = 6) on RD and HFD for 6 weeks.

See also Supplemental Figure S4.

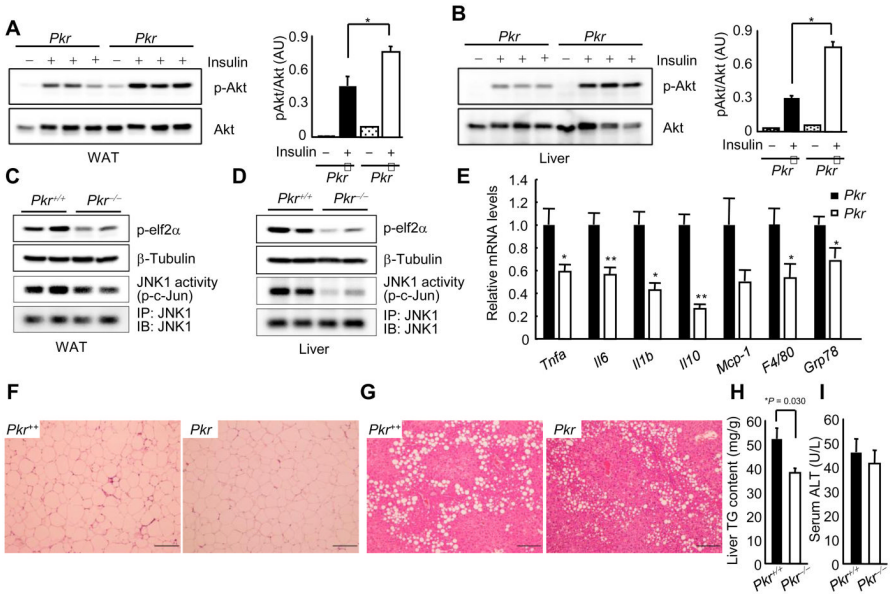

Figure 5. Biochemical and molecular alterations in *Pkr*$^{-/-}$ tissues

(A and B) Phosphorylation level of Akt on serine 473 in WAT (A) and liver (B) of *Pkr*$^{+/+}$ and *Pkr*$^{-/-}$ mice on HFD for 20 weeks. The graphs on the right of each blot show the quantification of the results. Data are shown as the mean ± SEM. **P*<0.05, ***P*<0.01. AU: Arbitrary unit.

(C and D) Phosphorylation level of eIF2α on serine 52 and JNK1 kinase activity, which was detected by a kinase assay using immunopurified JNK1, ATP [γ-32P] and recombinant c-Jun protein as substrate, in WAT (C) and liver (D) of *Pkr*$^{+/+}$ and *Pkr*$^{-/-}$ mice on HFD for 20 weeks. β-Tubulin is shown as a control.

(E) Gene expression in WAT including proinflammatory cytokine levels in *Pkr*$^{+/+}$ and *Pkr*$^{-/-}$ mice on HFD for 20 weeks.

(F and G) Haematoxylin and eosin staining of WAT (F) and liver (G) sections of *Pkr*$^{+/+}$ and *Pkr*$^{-/-}$ mice, respectively. Scale bar, 200 μm.

(H) Triglyceride contents in liver of *Pkr*$^{+/+}$ (*n* = 6) and *Pkr*$^{-/-}$ (*n* = 6) mice on HFD for 20 weeks.

(I) Serum alanine aminotransferase level after 6 hours daytime food withdrawal in *Pkr*$^{+/+}$ (*n* = 6) and *Pkr*$^{-/-}$ (*n* = 6) mice on HFD for 15 weeks. Data are shown as the mean ± SEM.

See also Supplemental Figure S5.

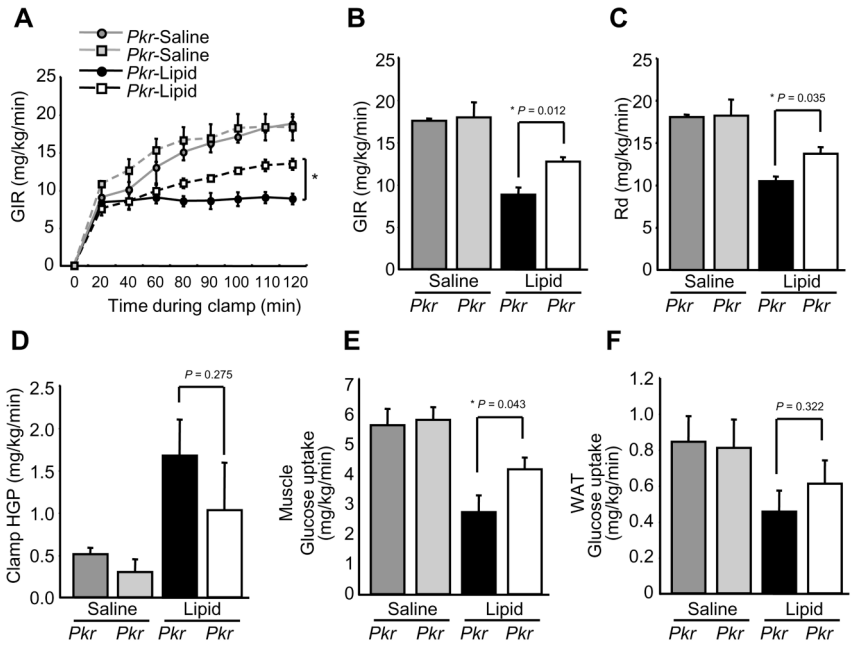

Figure 6. PKR mediates lipid-induced insulin resistance

(A–F) Hyperinsulinaemic–euglycaemic clamp studies performed in $Pkr^{+/+}$ (n = 5) and $Pkr^{-/-}$ mice (n = 5) infused with lipid for 5 hours. Glucose infusion rates (GIR) throughout the clamp procedure (A). Average GIR (B). Whole body glucose disposal rates (Rd) (C). Hepatic glucose production (HGP) during the clamp (D). Tissue glucose uptake in gastrocnemius muscle (E) and epididymal fat (F) tissues of $Pkr^{+/+}$ and $Pkr^{-/-}$ mice. Data are shown as the mean ± SEM.

See also Supplemental Figure S6.

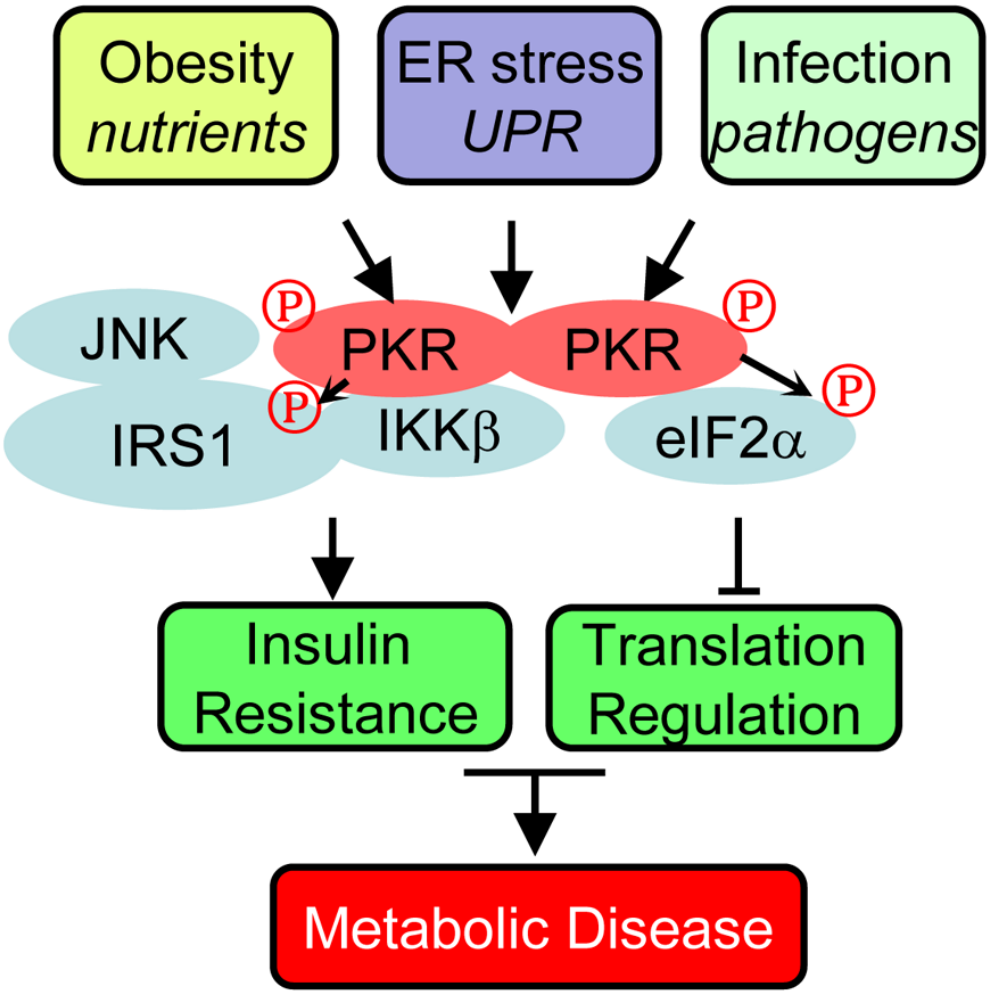

Figure 7. Regulation of systemic metabolic responses by PKR

PKR senses and responds to obesity, ER stress, and pathogen-related stress in concert with JNK, leading to metabolic disease under diverse physiological and pathological conditions. In this capacity, PKR not only integrates immune and metabolic response systems but also links endoplasmic reticulum homeostasis and unfolded protein response (UPR), to translational regulation through eIF2α and insulin signaling through IRS-1. Finally, the kinases, IRS-1 and eIF2α may represent a “metabolic inflammasome” complex assembled and regulated by PKR.